NRIAG JOURNAL OF ASTRONOMY AND GEOPHYSICS
2022, VOL. 11, NO. 1, 166–177
https://doi.org/10.1080/20909977.2022.2040174

Photometric and statistical comparisons of the old open cluster M67 (NGC 2682) using KFISP and Gaia EDR3 astrometry

Y.H.M. Hendy[a] and H. I. Abdel Rahman[b]

[a]Astronomy Department, National Research Institute of Astronomy and Geophysics, Cairo, EGYPT; [b]Astronomy Department, National Research Institute of Astronomy and Geophysics, Cairo, Egypt

ABSTRACT

We present the BV photometric observations of the open cluster M67 using the Kottamia Faint Imaging Spectro-Polarimeter (KFISP), mounted at the 74-inch telescope. We build three colour-magnitude diagrams of the Gaia EDR3 and the BV. We derived the photometric and astrometric parameters of the cluster. The mean parallax is 1.167 mas (distance is 857 ± 22 pc). The age and the reddening E(B-V) of the open cluster are 4.00 Gyr and 0.03 mag, respectively. We identified 434 members from the Gaia EDR3, with a probability >70%. The mean proper motion is obtained as $\mu_\alpha cos\delta = -10.98 \pm 0.28$ mas/yr and $\mu_\delta = -2.91 \pm 0.31$ mas/yr. We used statistical comparisons to test the quality of the observations taken from the KFISP. The statistical comparisons in the BV bands showed that there are no significant differences between observations and published catalogues.

ARTICLE HISTORY
Received 22 December 2021
Revised 3 February 2022
Accepted 6 February 2022

KEYWORDS
Open clusters; individual (M67) — stars; photometric and statistical comparisons

1. Introduction

Open star clusters are the basis to understand stellar evolution. Between them, M67 plays a special role. The old open cluster M67 (NGC 2682) has been the topic of many studies in the last 40 years. Gilliland et al. (1991; Stassun et al. 2002; van den Berg et al. 2002; Sandquist and Shetrone 2003a, 2003b; Stello et al. (2006); Stello et al. (2007), (Bruntt et al. 2007; Pribulla et al. 2008; Yakut et al. 2009) investigated variable stars inside the cluster. (Pasquini et al. 2012; Brucalassi et al. 2014) search for exoplanet candidates inside this cluster. The equatorial coordinates of the M67 are RA = 08 ^{h} 51 ^{m} 18^{s}.00 and DEC = +11° 48$'$ 00$''$.00, the Galactic coordinates are l = 215°.6961 and b = +31°.8963, and the angular diameter is 25 arcmin (Dias et al. 2002).

(Sanders 1977; Girard et al. 1989; Zhao et al. 1993; Yadav et al. 2008; Geller et al. 2015) calculated membership probability using a fitting model consisting of normal frequency functions on Vector Point Diagram (VPD). (Mathieu and Latham 1986; Mathieu et al. 1986, 1990; Milone 1992,; Milone and Latham 1994) calculated the radial velocities. Pasquini et al. (2011) found the radial velocity (RV) of the cluster M67 is RV = 33.74 ± 0.12 km/s, velocity dispersion is 0.54 and 0.68 km/s for giants and dwarfs, respectively, which in both cases is substantially lower than reported in previous works.

(Janes and Smith 1984; Montgomery et al. 1993; Nardiello et al. 2016) estimated the cluster age is 4.00 Gyr. Taylor (2007) calculated the reddening E (B-V) = 0.041 ± 0.004. Percival and Salaris (2003) measured the metallicity [Fe/H] = 0.02 ± 0.06, E (B-V) = 0.04 ± 0.02, and distance modulus $(m - M)_o$ = 9.60 ± 0.09.

Cantat-Gaudin et al. (2020) by using Gaia DR2 determined that mean proper motions $(\overline{\mu_\alpha cos\delta}, \overline{\mu_\alpha}) = (-10.99 \pm 0.19, -2.96 \pm 0.20)$ mas/yr, the mean parallax $\bar{\pi} = 1.14 \pm 0.05$ mas, log(age) = 9.63, and the distance is 889 pc. Spina et al. (2021) by using the surveys of both GALactic Archaeology with HERMES (GALAH) and the Apache Point Observatory Galactic Evolution Experiment (APOGEE) determined the log(age) = 9.63 yr, distance is 882 ± 42 pc, $\bar{\pi} = 1.14 \pm 0.05$ mas, and $(\overline{\mu_\alpha cos\delta}, \overline{\mu_\alpha}) = (-10.99 \pm 0.21, -2.96 \pm 0.22)$ mas/yr.

For Gaia DR2, sources with G < 13 mag the photometric uncertainties are 0.3, 2, 2 mmag of G, G_{BP} and G_{RP} respectively. For sources G < 17 mag the photometric uncertainties are 2, 10, 10 mmag of G, $G_{BP,}$ and G_{RP} respectively. For sources G < 20 mag the photometric uncertainties are 10, 200, 200 mmag of G, $G_{BP,}$ and G_{RP} respectively (Gaia Collaboration et al. 2018). For Gaia EDR3, sources with G < 13 mag the photometric uncertainties are 0.3, 0.9, 0.6 mmag of G, $G_{BP,}$ and G_{RP} respectively. For sources G < 17 mag the photometric uncertainties are 1, 12, 6 mmag of G, $G_{BP,}$ and G_{RP} respectively. For sources G < 20 mag the photometric uncertainties are 6, 108, 52 mmag of G, $G_{BP,}$ and G_{RP} respectively (Gaia Collaboration et al. 2021). The photometric limit of the passbands used

CONTACT H. I. Abdel Rahman helal_ismaeil@yahoo.com National Research Institute of Astronomy and Geophysics (Nriag), Cairo, Egypt

(G, G_{BP}, G_{RP}) of the Gaia EDR3, corresponding photometric errors, and completeness is in a high-quality better than Gaia DR2.

This work aims to test the quality of the observations from the Kottamia Faint Imaging Spectro-Polarimeter (KFISP) of the 74-inch telescope, Egypt. Determination of physical parameters of the standard open cluster M67 using the high-quality of the astrometry from the latest version of the Gaia telescope, Gaia EDR3, and the BV observations taken from the KFISP. Then compare with previous studies. We used the statistical comparisons between our observations and the available data from the literature to test the quality and deviations from the published literature.

We used three CMDs of the Gaia EDR3 and the BV CCD observations of the KFISP. We determined the distance (astrometry) of the cluster using high-quality parallax from the Gaia EDR3 and three CMDs (photometry). Observations and CCD calibration data are presented in Section 2. The membership, photometric, and physical parameters are explained in Section 3. The statistical comparisons methods and discussions between our BV magnitudes and the published photometric data are described in Section 4. The conclusions are presented in Section 5.

Table 1. Log of optical observations of M67 is given along with the date, exposure time in seconds, airmass, and seeing in each filter.

Date	Filter	Exposure Time	Airmass	Seeing
28 January 2020	B	3x60	1.08	1.4
	V	3x15	1.08	1.3

2. Observations and CCD calibration data

The charge coupled device (CCD) photometric observations of the open cluster M67 in the B and V bands were obtained using the KFISP. The KFISP is mounted at the Cassegrain focus of the 74-inch telescope of the Kottamia Astronomical Observatory (KAO), Egypt (Azzam et al. 2020 & Azzam et al. 2021). The observations were taken on 28 January 2020 with an exposure time of 3 × 60 and 3 × 15 s in the B and V bands, respectively. The CCD (2k x 2k) of the direct imaging mode has a field of view of 8 × 8 arcmins and the pixel scale is 0.25 arcsec/pixel. The mean seeing is 1.4 and 1.3 arc seconds in the B and V bands, respectively, while the mean air mass is 1.08 in B & V (Table 1).

The CCD data were observed with one amplifier, the basic reduction of CCD frames was corrected by using the IRAF's code (Hendy and Bisht 2021). The sky map for M67 in V-band is shown in Figure 1.

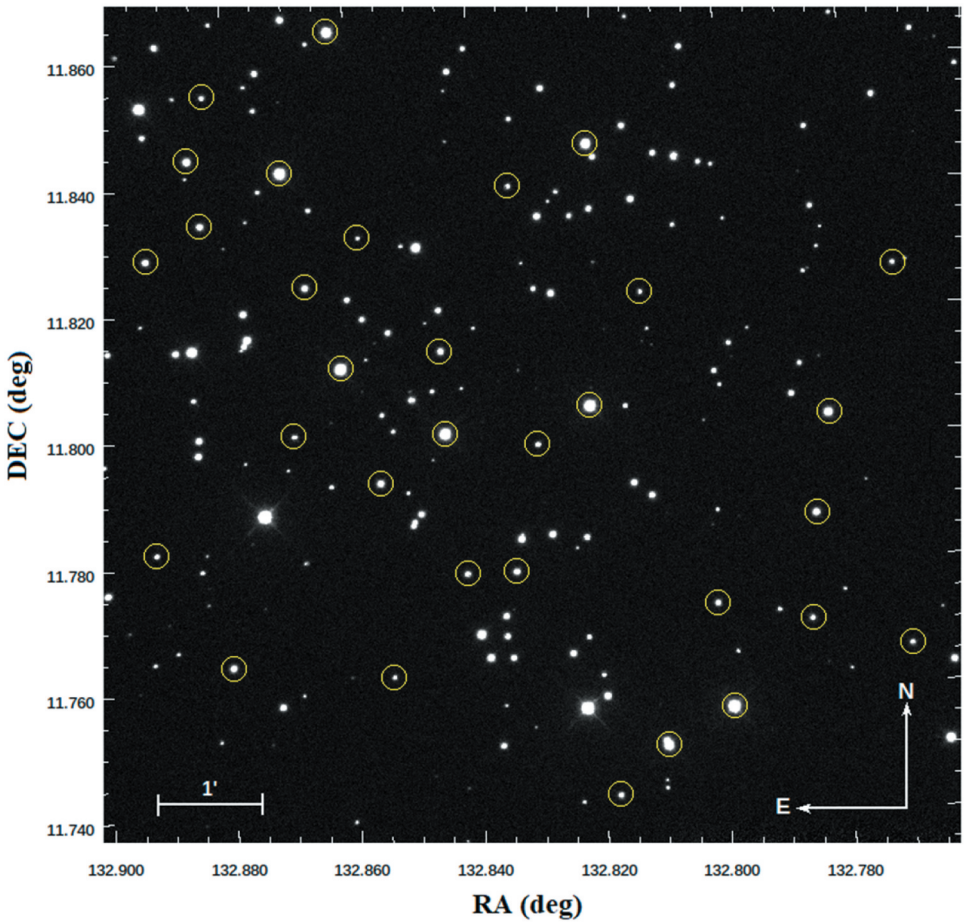

Figure 1. The sky map of the stars in the field of open cluster M67 in the V-band taken with 74-inch telescope of the KAO. The yellow circles represent the 32 stars taken from the APASS catalogue to obtain standard magnitude.

To obtain instrumental magnitude, we used the Point Spread Function (PSF) of the DAOPHOT package on the IRAF (Stetson 1987&1992). We used several isolated stars not saturated and distributed over the entire CCD to obtain good photometric results. We used aperture corrections of isolated and unsaturated bright stars in the CCD frame.

To convert instrumental magnitude into standard magnitude, we cross-identified stars in BV observed data with the APASS catalogue (Henden et al. 2016), we obtained 32 stars, see the yellow circles in Figure 1. We used the calibration curves to convert the instrumental magnitude to the standard magnitude V_{APASS}, see Figure 2. We obtained the linear fitting $B_{APASS} = 0.9998\ B_{inst} - 1.3369$ and $V_{APASS} = 1.0075\ V_{inst} - 1.8147$ with a correlation coefficient are 0.99.

We obtained a standard magnitude of 245 stars in the B and V bands. The mean error in the V is 0.1 at V ~ 19.5 mag, Figure 3. To compare our measurement of BV bands with previous photometry in the literature, we cross-identified our BV with Montgomery et al. (1993) (hereafter MONT), Nardiello et al. (2016) (hereafter NARD), Stassun et al. (2002) (hereafter STAS), and Yadav et al. (2008) (hereafter YADA), we found 102, 42, 19, and 42 stars, respectively, Figure 4. The mean difference between our B & V and the previous photometry of Montgomery et al. (1993), Nardiello et al. (2016), Stassun et al. (2002), and Yadav et al. (2008) <0.1 magnitude.

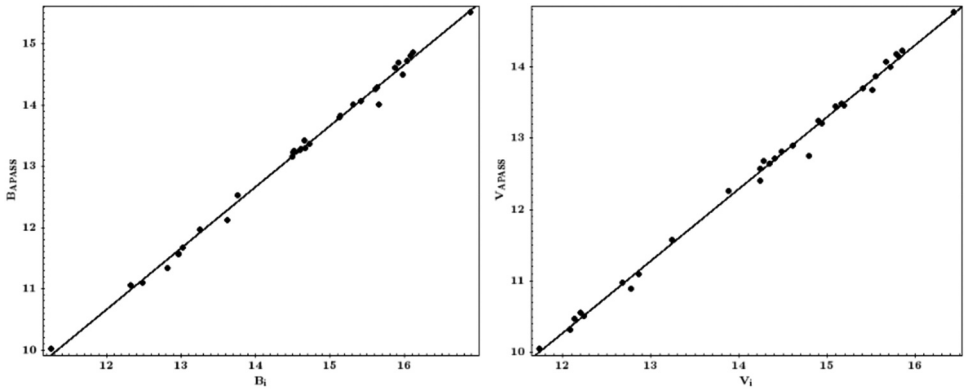

Figure 2. Calibration curves to convert the instrumental magnitude B_{inst} and V_{inst} to the standard magnitudes.

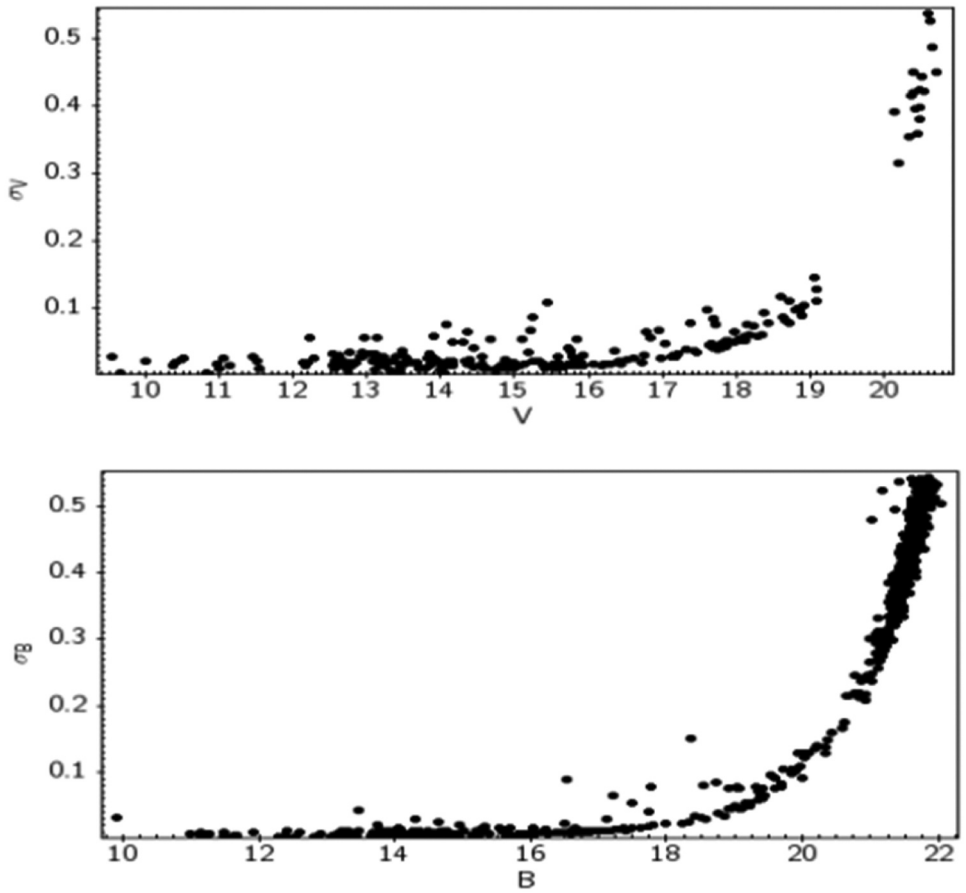

Figure 3. Photometric errors in the B and V bands.

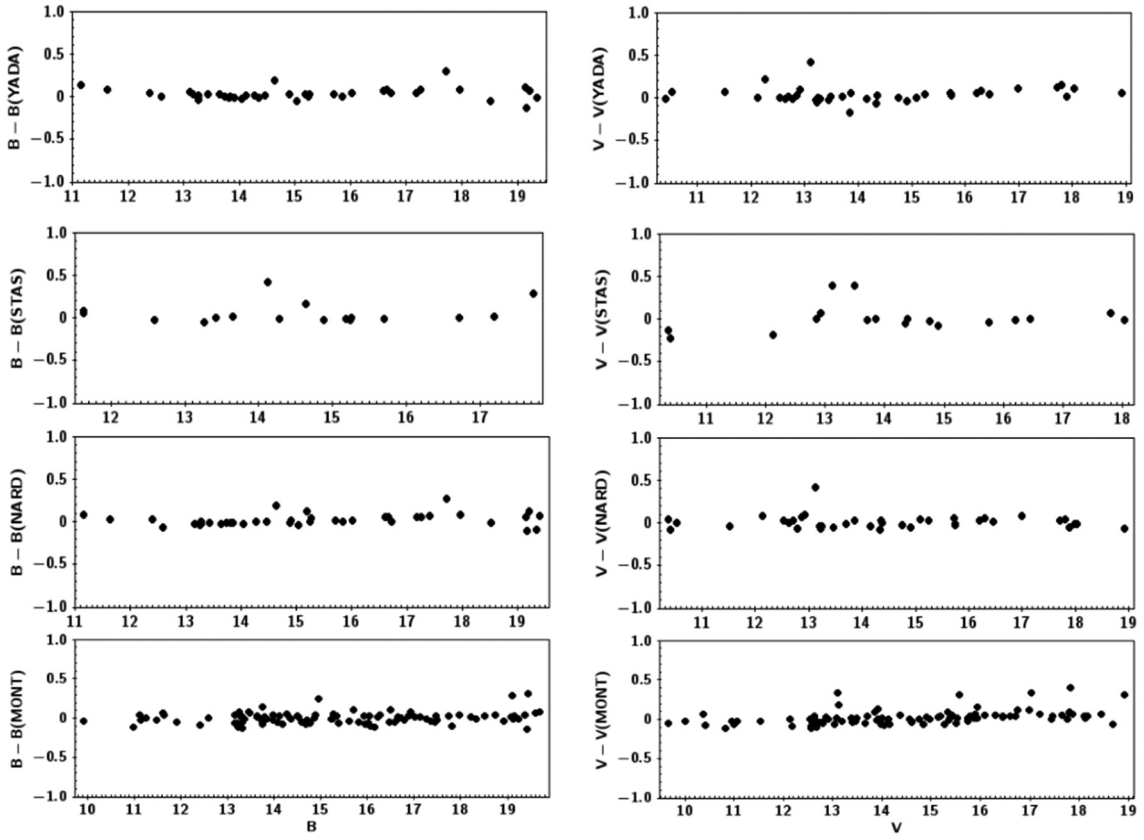

Figure 4. Differences between our results of B and V using KFISP/KAO and the published of **MONT** (montgomery et al. 1993); **NARD** (Nardiello et al. 2016); **STAS** (Stassun et al. 2002); **YADA** (Yadav et al. 2008).

3. The membership, photometric, and physical parameters

We searched in the Gaia EDR3 (Gaia Collaboration et al. 2021) using a large radius within our criteria, the maximum radius is 3 r_{50} ~ 30 arcmins. The r_{50} is the radius containing half the members (Cantat-Gaudin et al. 2018). We present the photometric errors in the G-mag in Figure 5, the maximum error is 0.015 mag. The distributions of proper motions and their errors with G-mag are displayed in Figure 6.

Proper motions have an important role to remove field stars from the main sequence of an open cluster (Hendy and Bisht 2021). To obtain a good quality from the astrometric data of Gaia EDR3, we remove the stars with the error of the parallax and proper motions >0.5. We used the Vector Point Diagram (VPD) of the proper motions ($\mu_\alpha cos\delta$ & μ_δ) to select the over-density region of the open cluster M67. We selected 591 candidate member stars inside the red box. These candidates show a good trend with parallax and parallax error Figure 7.

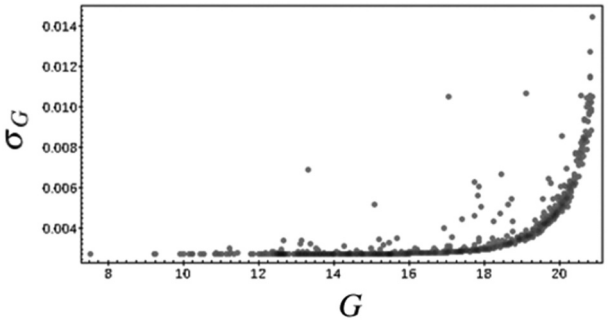

Figure 5. Photometric errors in the G band against G.

To obtain membership probabilities of stars in the M67, we remove the stars with proper motions and parallax larger than 3 Median Absolute Deviation (MAD) from the median proper motions and median parallax of the M67. We obtained 434 member stars from Gaia EDR3, with membership probability >70% in Cantat-Gaudin et al. (2018). The CMD of the Gaia EDR3 and the combined CMD of V-mag and the colour (G_{BP} _ G_{RP}) show a good trace of the main sequence. The co-moving member stars move in the same direction in the space (Figure 8).

The mean value of the parallax, proper motions are $\bar{\pi} = 1.15 \pm 0.03$ mas and $(\overline{\mu_\alpha cos\delta}, \overline{\mu_\alpha}) = (-10.98 \pm 0.28, -2.91 \pm 0.31)$ mas/yr. The total proper motion $\mu = \sqrt{(\mu_\alpha \cos\delta)^2 + (\mu_\delta)^2}$ is 11.36 ± 0.42 mas/yr.

We plot the histogram of the values of parallax with a bin size of 0.01 in Figure 9, while the histogram of the proper motions is $\mu_\alpha cos\delta$ and μ_δ

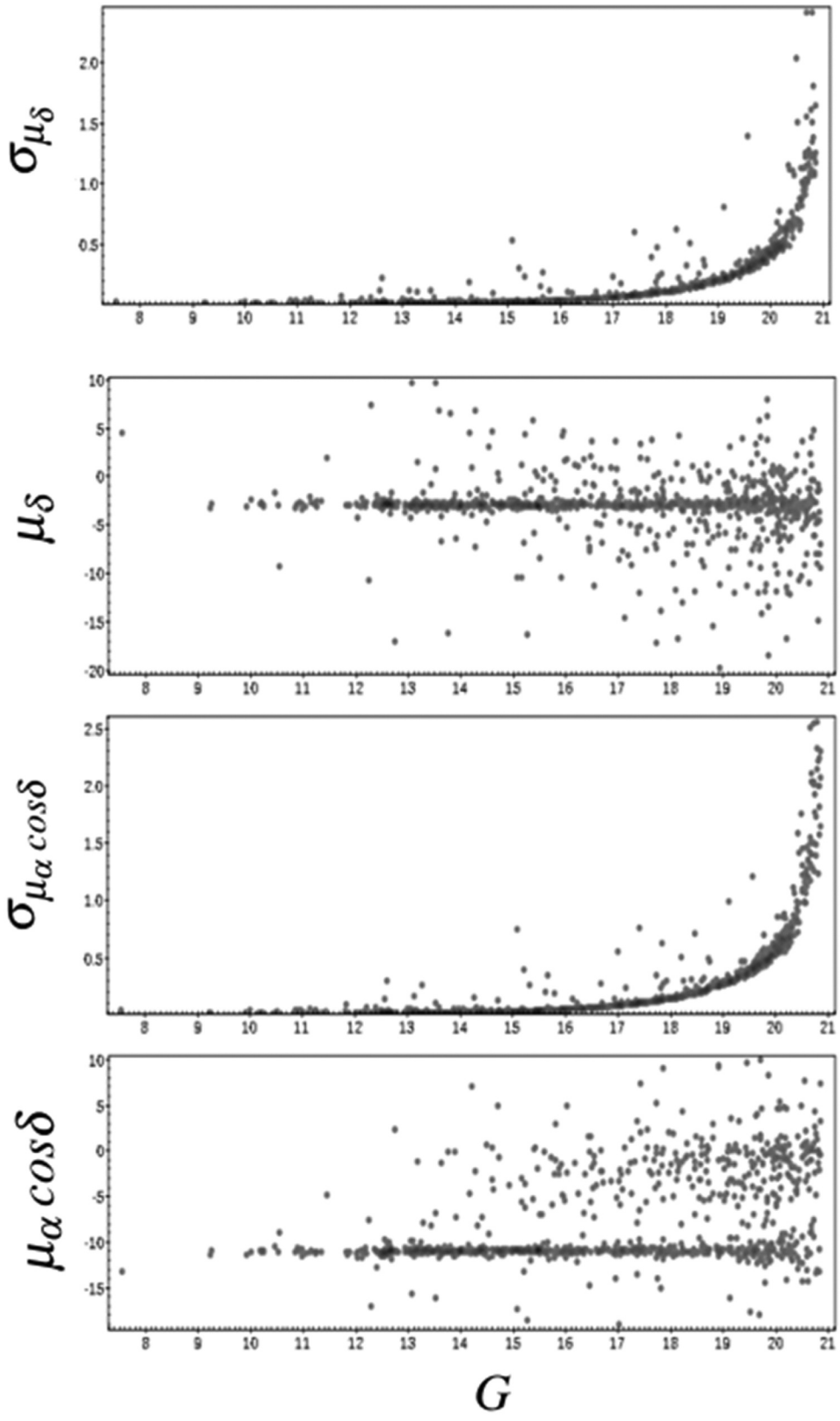

Figure 6. The proper motions in both directions with errors versus G.

with a bin size of 0.1 in Figure 10. The mean value of the centre of the open cluster M67, RA is 132.84 ± 0.07 degrees and DEC is 11.81 ± 0.07 degrees, Figure 11.

We used the three CMDs of the Gaia EDR3, the combined CMD of the V-mag and the colour (G_{BP} – G_{RP}), and the CMD V (B-V) to obtain the best fitting of the age, distance modulus, and the reddening,

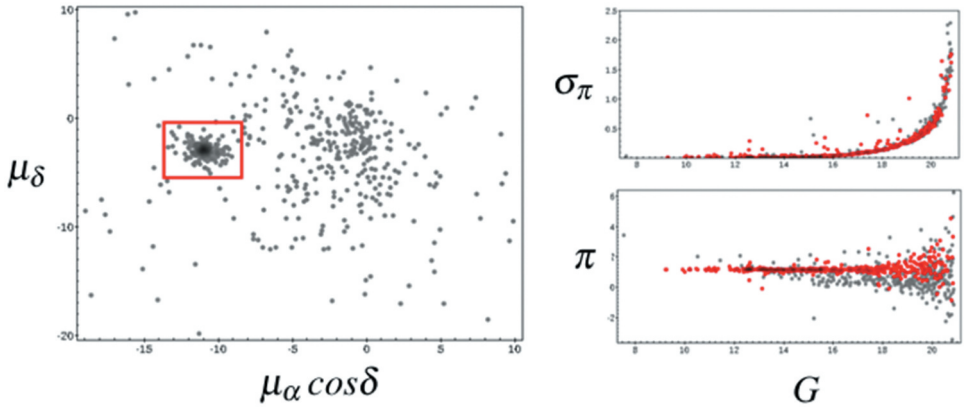

Figure 7. The left panel represents the Vector Point Diagram (VPD). The red box defines the cluster region of the M67. The right panel represents the parallax and parallax error against G-mag, the probable members have red circles, and the field stars have grey circles.

Figure 12. We apply the recent value of the solar metallicity Z = 0.0152 to adopt the isochrones of Bressan et al. (2012). The best fitting of isochrones of the log (age) is 9.60 ±0.05 (i.e. age is 4.00 Gyr).

We used the transformation equations of Cardelli et al. (1989) & O'Donnell (1994), $A_G = 1.86\ E(G_{BP} - G_{RP})$ and $E(B\text{-}V) = 0.72\ E(G_{BP} - G_{RP})$ to obtain the extinction A_G and the reddening E(B-V). The true distance modulus $(m\text{-}M)_0$ and the reddening E(B-V) is 9.5 mag and 0.04 mag respectively.

The photometric distance of the M67 $d_{photometric}$ = 802 ±36 pc. The correcting of mean parallax is 1.167 mas with the offset 0.017 of Lindegren et al. (2021). This led to the distance from inverting parallax $d_{astrometric}$ = 857 ±22 pc. This is in good agreement with our fitting. Our measurements of the centre, mean parallax, mean proper motion in RA and DEC, distance, age, and reddening are in very good agreement with the literature, see Table 2.

Table 2. The physical parametric of the open cluster M67.

Parameters	Value	Reference
RA (deg)	132.85 ±0.07	Our study
	132.85	CG2020
DEC (deg)	11.82 ±0.07	Our study
	11.81	CG2020
$\bar{\pi}$ (mas)	1.15 ±0.03	Our study
	1.14 ±0.05	SP2021
	1.14 ±0.05	CG2020
$\overline{\mu_{\alpha\cos\delta}}$ (mas/yr)	−10.98 ±0.28	Our study
	−10.99 ±0.21	SP2021
	−10.99 ±0.19	CG2020
$\overline{\mu_\delta}$ (mas/yr)	−2.91 ±0.31	Our study
	−2.96 ±0.22	SP2021
	−2.96 ±0.20	CG2020
$d_{astrometric}$ (pc)	857 ±22	Our study
	882	SP2021
	859	Mo2020
$d_{photometric}$ (pc)	802 ±36	Our study
	855	Mo2020
	889	CG2020
log age	9.60 ±0.05	Our study
	9.63	SP2021
	9.56	Mo2020
	9.63	CG2020
$E(G_{BP} - G_{RP})$	0.04	Our study
E(B-V)	0.04	Our study
	0.06	Mo2020
	0.02	CG2020

CG2020: Cantat-Gaudin et al. (2020); SP2021: Spina et al. (2021); Mo2020: Monteiro et al. 2020)

4. Statistical comparisons methods and discussions between our BV magnitudes and the published photometric data

We compared our BV bands observations of the same stars in the open cluster M67 with the same stars in published catalogues as listed in Table 3. The comparison is based on the correlation coefficients and statistical testing hypothesis by independent Samples T-Test.

4.1. The correlation coefficients

First, we examined the correlation coefficients between the V-band observations and the previous studies for M67. We calculated these correlations by the Pearson's correlation coefficient (Bobko 2001) from the next formula as follows:

$$r = \frac{cov(x,y)}{\sigma_x \sigma_y} \quad (1)$$

where r is the correlation coefficient between the populations x and y.

cov(x,y) is the covariance between populations.

σ_x and σ_y are the standard deviations for the populations

Table 3. The sample sizes of stars and the correlation coefficients (r) between our observations and different authors.

	MONT	NARD	STAS	YADA
r between B-mag and other authors	99.80%	100 %	98.70%	99.90%
r between V-mag and other authors	99.30 %	99.60%	99.20 %	99.60 %
Sample sizes of stars combined with us	102	42	19	42

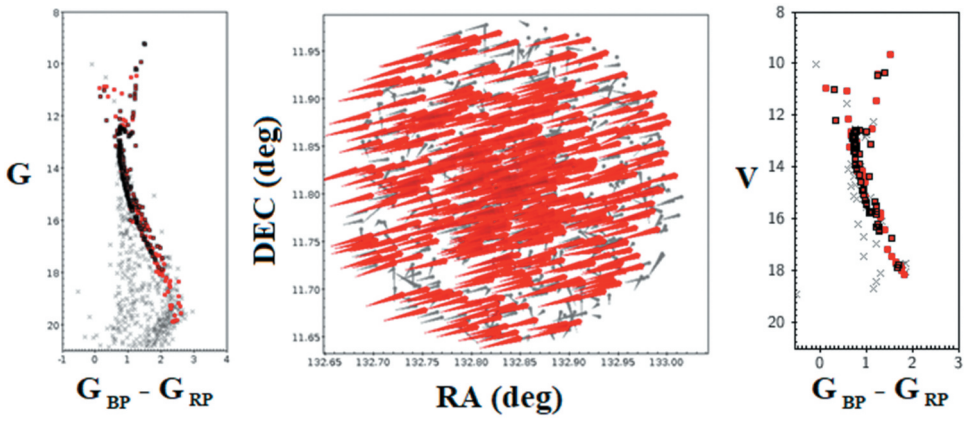

Figure 8. The left panel represents the CMD of the Gaia EDR3, and the medium panel represents the co-moving member stars (i.e. the stars that travel together in the same direction through space). The right panel represents the combined CMD of the V-mag measured from the KFISP/KAO instrument and the colour (BP-RP) taken from the Gaia EDR3. The member stars have red colours and the field stars have grey colours.

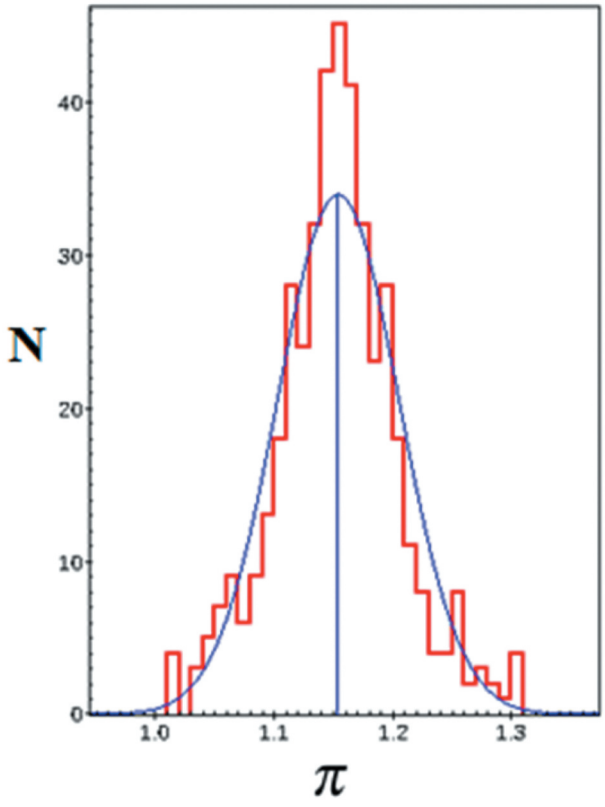

Figure 9. Histogram and Gaussian fitting of the parallax.

Table 3 contains the sample sizes of stars combined with us and Pearson's linear correlation coefficients (r) between our observations of B and V bands and the previous studies. These correlation coefficients are calculated by applying equation (1). The correlation coefficient between our observations of BV bands and the previous studies is very strong, which is equal to 99.80%, 100%, 98.70%, and 99.90% in B-mag and 99.30%, 99.60%, 99.20%, and 99.60% in V-mag as listed in Table 3.

Second, by an independent statistical T-Test for comparing equal population means. This method depends on basic assumptions such as the samples being independent of each other. The population of observations from which the sample was taken follows a Gaussian (normal) distribution and the sampled populations have homogeneous variances.

The next step is to confirm the comparison using the testing hypothesis. To apply the independent statistical T-Test, it is necessary to verify the previous assumptions and see whether they are fulfiled or not given that the first of the three conditions are fulfiled.

4.2. Test of normality

There are different methods to test the normality of the data. The common methods are the two tests Kolmogorov–Smirnov (K-S) and the Shapiro–Wilk (W).

- ***First***: The **(K-S) test**

Null hypothesis, $\mathbf{H_0}$: The observational data follow a normal (Gaussian) distribution.

Alternative hypothesis, $\mathbf{H_1}$: The observational data do not follow a normal (Gaussian) distribution.

Test Statistic: The relation of **(K-S)** test statistic is defined as (Chakravarty et al. 1967)

$$K_s = \max_{1\le j\le n}\left[F(Y_j) - \frac{j-1}{N}, \frac{j}{N} - F(Y_j)\right] \qquad (2)$$

Where $\boldsymbol{F}$ is the cumulative normal (Gaussian) distribution function.

The normality hypothesis is accepted H_0 if the test statistic, K_s is smaller than the critical value obtained from the K-S table.

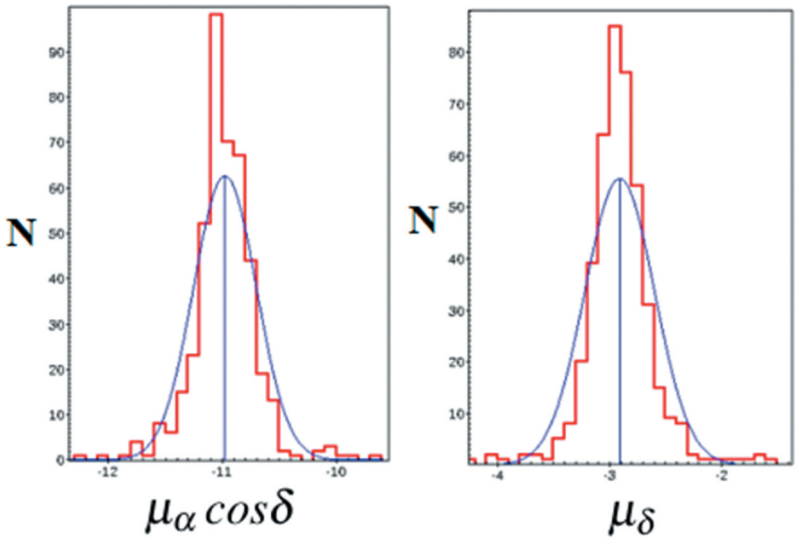

Figure 10. Histogram and Gaussian fitting of the proper motions ($\mu_a cos\delta$ and μ_δ).

The statistical programs have used the probability value (p-value) to determine the critical region for rejection or acceptance of the null hypothesis, where the p-value is the probability of getting results close to the real ones, assuming that the null hypothesis is true. We will use this value in all our results.

***Second*: The W test**

The Shapiro–Wilk test is denoted by W, The W statistic is calculated from the next formula (3) (Chakravarty et al. 1967):

$$W = \frac{\left(\sum_{i=1}^{n} a_i X_{(i)}\right)^2}{\sum_{i=1}^{n} \left(X_i - \overline{X}\right)^2} \quad (3)$$

where the $x_{(i)}$ is the ordered sample values and the a_i are constants generated from the central tendency and dispersion measures of sample size (n) taken from a Gaussian distribution. We compared with the tabulated value that was reproduced by (Pearson and Hartley 1972) or by using the p-value.

The first condition for applying the Independent Sample T-Test is to test the normality between the different populations under test. We apply the two Equations (2) and (3), we get Table 4 for our observations and different authors.

The significant level (α = 0.05) is smaller than the p-value in column 2 (Kolmogorov-Smirnov) and column 3 (Shapiro-Wilk) as shown in Table 4. Then, we cannot reject H_0 that all populations follow a normal (Gaussian) distribution.

4.3. Test of homogeneity

Homogeneity means variance between the groups as equals, *Levene's* test is used to test the homogeneity between populations (Levene1960). If the resulting

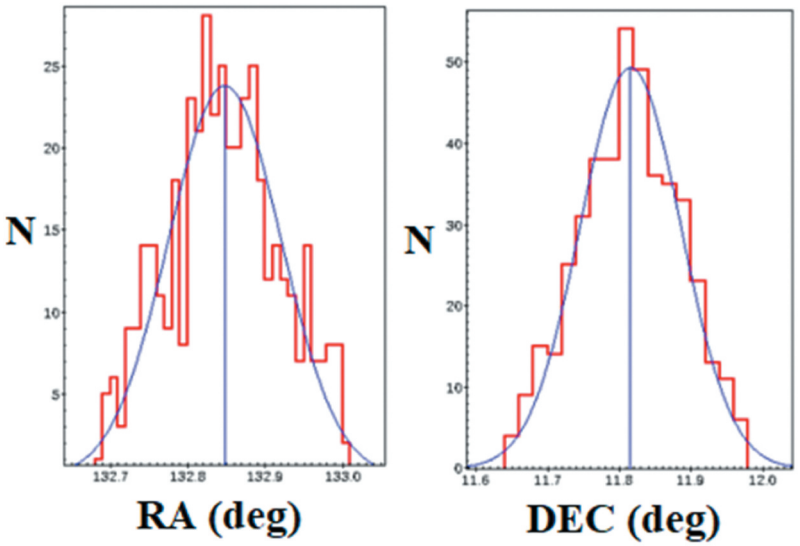

Figure 11. Histogram and Gaussian fitting of the RA and DEC.

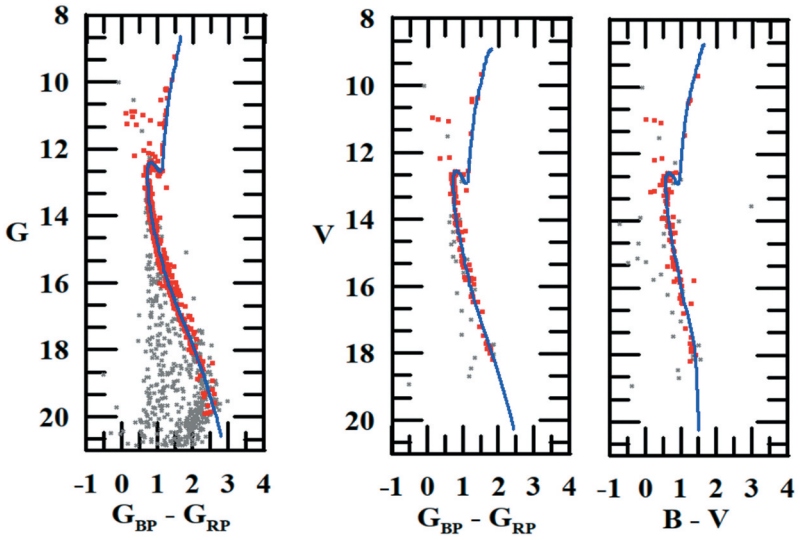

Figure 12. The CMDs (G and $G_{BP} - G_{RP}$), and (V, $G_{BP} - G_{RP}$, and B-V).

probability value (p-value) of this test is less than some significant level (0.05), the null hypothesis of equal variances will be rejected and there is a difference between the variances in these observations.

The steps of the test are the following:

The Statistical hypothesis

H_0: The variances are homogenous in two populations.

$$H_0 : \sigma_1^2 = \sigma_2^2$$

H_1: The variances are heterogeneous in two populations.

$$H_1 : \sigma_1^2 \neq \sigma_2^2$$

Statistic test

If the size of the observations is N concerning the Y variable and divided into K subgroups and the size of the i-th subgroup is N_i, the Levene test statistic is described as follows:

$$L = \frac{(N-k)}{(k-1)} \frac{\sum^{i} = 1^{k} (\bar{Z}_{i.} - \bar{Z})^2}{\sum_i = 1^{k} (Z_{ij} - \bar{Z}_i)^2} \quad (4)$$

where

$$Z_{ij} = Y_{ij} - \bar{Y}_{i.} \quad (5)$$

where

$\bar{Y}_i$ is the mean of the i-th subgroup.

and $\bar{Z}_i$ are the means group of the $\boldsymbol{Z_{ij}}$ and $\bar{Z}$ is the overall mean of the $\boldsymbol{Z_{i.}}$

Critical region

The Levene's test rejects the null hypothesis that the variances are equal if

$$L > F_{\alpha,k-1,N-k} \quad (6)$$

where $F_{\alpha,\ k-1,\ N\text{-}k}$ is the F distribution with degrees of freedom k-1 and N-k at a significant level of α.

We used equation (4) to get Table 5. We find that the p-value of the Levene test is greater than the significant level (α = 0.05), so we cannot reject the null hypothesis. Then, the variances are equal between these populations.

4.4. The independent sample T-Test

After confirming the validity of the data test fulfiling the normal distribution and homogeneity, we compared between BV observations and four published catalogues in different observatories for cluster M67 by independent Samples T-Test. We

Table 4. Test of normality between our BV bands and different authors.

Authors	BV bands	p-value (K-S)	p-value (W)
MONT	B	0.128	0.37
	V	0.200	0.157
STAS	B	0.200	0.755
	V	0.200	0.625
NARD	B	0.200	0.139
	V	0.200	0.504
YADA	B	0.048	0.067
	V	0.200	0.377

Table 5. Levene's Test between the different populations.

Authors	BV bands	p-value (Levene Statistic)
MONT	B	0.978
	V	0.962
STAS	B	0.754
	V	0.493
NARD	B	0.953
	V	0.947
YADA	B	0.967
	V	0.923

Table 6. The comparison between our observations and four authors.

Authors	BV bands	T (Calculated)	p-value (Independent Samples Test)
MONT	B	0.039	0.969
	V	0.238	0.812
STAS	B	0.277	0.784
	V	0.733	0.469
NARD	B	0.042	0.966
	V	0.122	0.903
YADA	B	0.062	0.951
	V	0.158	0.875

compared the mean of observations of BV bands with each of the other four observatories to determine whether there is a significant difference between the means in two independent groups.

The T-Test is the test statistic of the statistical hypothesis test and follows the student T-distribution under the hypothesis of the study. We explain the steps of testing the hypothesis for means μ.

- The steps of statistical testing hypothesis (Abdel-Rahman et al. 2017)

I- Hypothesis of study

$H_0 : \mu_1 = \mu_2$ and $H_1 : \mu_1 \neq \mu_2$

II- Significant level $\alpha = 0.05$

iii- Statistic test

The t statistic is calculated from the following equation:

$$T = \frac{\bar{X}_1 - \bar{X}_2}{S_p \sqrt{\frac{2}{n}}} \tag{7}$$

where $\bar{X}_1$ and $\bar{X}_2$ are the means of two samples.

And

$$S_p = \sqrt{\frac{S_1^2 + S_2^2}{2}} \tag{8}$$

S_p^2 is the pooled variance of equal size for the two samples ($n_1 = n_2$) and S_2^2, S_2^2 are the variances of the two samples.

Iv- Critical region

we reject the null hypothesis, if the statistical test is located in the rejection or acceptance region, or the P-value is smaller than the significant level α = 0.05.

V- The decision

We can reject or accept H_0 according to the last step (iv).

We apply Equations (7) and (8) to calculate the statistical T-Test. Table 6 reveals the comparison between our observations and other studies.

The most important column in Table 6 is the third because it is the decisive factor to determine the acceptance or rejection of the hypothesis. The p-value is greater than the significant level (0.05) with all the previous studies. Thus, we cannot reject the null hypothesis that there is no significant difference between our study and the other studies.

5. Conclusions

We presented the physical parametric study of the old open cluster M67 using the CCD BV-bands of the Kottamia Faint Imaging Spectro-Polarimeter (KFISP) and the Gaia EDR3. We estimated the 434 members using the Gaia EDR3, with a membership probability higher than 70%. We used those members to obtain the photometric and astrometric parameters. These measurements of the parameters are in very good agreement with published results, Table 2. We determined the distance using the inverting parallax ($d_{astrometric}$ = 857 ± 22 pc) from Gaia EDR3 and using three CMDs of Gaia EDR3 and BV CCD observations ($d_{photometric}$ = 802 ± 36 pc). The correlation coefficients between our measurements of the BV bands and the others are very strong correlation. The normality and homogeneity for the KFISP observations of all populations show the normal (Gaussian) distribution and equal variances (homogeneity). The T-Test showed that there are no significant differences between BV observations and published results. This means that the observations of KFISP are consistent with the published catalogues of photometric data in BV bands.

Acknowledgements

The authors are deeply thankful to the referee for his/her valuable and constructive comments that improved the original manuscript. We thank our colleagues Prof. Ashraf Latif, Prof. Mohamed Nouh, and Prof. Magdy Sanad for their comments and the discussions to improve this paper. We thank our colleague's Prof. Yosry Azzam and Dr. Ibrahim Zead for helping to

take the observations using KFISP/KAO instrument. This work made use of data from the European Space Agency (ESA) mission Gaia (https://www.cosmos.esa.int/web/gaia/early-data-release-3) This work made use of TOPCAT (http://www.starlink.ac.uk/topcat) This work made use of data from the American Association of Variable Star Observers (AAVSO) Photometric All-Sky Survey APASS catalog.

Disclosure statement

No potential conflict of interest was reported by the author(s).

References

Abdel-Rahman HI, Nouh MI, Elsanhoury WH, 2017, Astrophysical bulletin, 72, 199.

Azzam YA, Ali GB, Elnagahy FIY, Zead, I, Ahmed, NM, Ismail, Hamed, Saad, Somaya, Shokry, A, Takey, Ali, Hendy, YHM, et al., 2020, In: Proc. SPIE 11447, Ground-based and Airborne Instrumentation for Astronomy VIII, 114479U.doi: 10.1117/12.2561664.

Azzam YA, Elnagahy FIY, Ali GB, Essam, A, Saad, Somaya, Ismail, Hamed, Zead, I, Ahmed, NM, Yoshida, Michitoshi, Kawabata, KS, et al. 2021. Experimental astronomy. 23:45–70. doi:10.1007/s10686-021-09802-z.

Bobko P. 2001. Correlation and regression: applications for industrial organizational psychology and management. 2nd ed. Thousand Oaks (CA): Sage Publications.

Bressan A, Marigo P, Girardi L, Salasnich B, Dal Cero C, Rubele S, Nanni A. 2012. Parsec: stellar tracks and isochrones with the PAdova and TRieste stellar evolution code. MNRAS. 427:127. doi:10.1111/j.1365-2966.2012.21948.x.

Brucalassi A, Pasquini, L, Saglia, R, Ruiz, MT, Bonifacio, P, Bedin, LR, Biazzo, K, Melo, C, Lovis, C, Randich, S, 2014. A&A. 561:L9. https://doi.org/10.1051/0004-6361/201322584

Bruntt H, Stello D, Suarez JC, Arentoft T, Bedding TR, Bouzid MY, Csubry Z, Dall TH, Dind ZE, Frandsen S, et al. 2007. Multisite campaign on the open cluster M67 - III. Scuti pulsations in the blue stragglers. MNRAS. 378:1371. doi:10.1111/j.1365-2966.2007.11865.x.

Cantat-Gaudin T, Anders F, Castro-Ginard A, Jordi, C, Romero-Gómez, M, Soubiran, C, Casamiquela, L, Tarricq, Y, Moitinho, A, Vallenari, A, et al. 2020. A&A. 640:A1. https://doi.org/10.1051/0004-6361/202038192

Cantat-Gaudin T, Jordi C, Vallenari A, Ramos S, Homem V, Ratola N, Carreras H. 2018. A&A. The Science of the Total Environment. 618:93. doi:10.1016/j.scitotenv.2017.10.295.

Cardelli JA, Clayton GC, Mathis JS. 1989. The relationship between infrared, optical, and ultraviolet extinction. ApJ. 345:245. doi:10.1086/167900.

Chakravarty IM, Laha RG, and Roy J. 1967. Handbook of methods of applied statistics. Volume I: Techniques of Computation Descriptive Methods, and Statistical Inference. Volume II: Planning of Surveys and Experiments. New York: John Wiley.

Dias WS, Alessi BS, Moitinho A, and Lepine JRD. 2002. A&A. 389:871–873. doi:10.1051/0004-6361:20020668.

Gaia Collaboration, et al. 2018. A&A. 616:A1.

Gaia Collaboration, et al. May 2021. A&A. 649:A1.

Geller AM, Latham DW, Mathieu RD. 2015. STELLAR RADIAL VELOCITIES IN THE OLD OPEN CLUSTER M67 (NGC 2682). I. MEMBERSHIPS, BINARIES, AND KINEMATICS. AJ. 150:97. doi:10.1088/0004-6256/150/3/97.

Gilliland RL, Brown TM, Duncan DK, Suntzeff NB, Lockwood GW, Thompson DT, Schild RE, Jeffrey WA, Penprase BE. 1991. Time-resolved CCD photometry of an ensemble of stars in the open cluster M67. AJ. 101:541. doi:10.1086/115703.

Girard TM, Grundy WM, Lopez CE, van Altena WF. 1989. Relative proper motions and the stellar velocity dispersion of the open cluster M67. AJ. 98:227. doi:10.1086/115139.

Henden AA, Templeton M, Terrell D, Smith, TC, Levine, S, Welch, D, 2016. VizieR online data catalog: II/336. 2015AAS:22533616H .

Hendy YHM, Bisht D. 2021. STUDY OF AN INTERMEDIATE AGE OPEN CLUSTER IC 1434 USING GROUND-BASED IMAGING AND GAIA DR2 ASTROMETRY. Revista Mexicana de Astronomía Y Astrofísica. 57:381. doi:10.22201/ia.01851101p.2021.57.02.10.

Janes KA, Smith GH. 1984. The giant branch of the old open cluster M67. AJ. 89:487. doi:10.1086/113539.

Lindegren L, Bastian U, Biermann M, Bombrun, A, de Torres, A, Gerlach, E, Geyer, R, Hernández, J, Hilger, T, Hobbs, D, et al. 2021. A&A. 649:A4. https://doi.org/10.1051/0004-6361/202039653

Mathieu RD, Latham DW. 1986. The spatial distribution of spectroscopic binaries and blue stragglers in the open cluster M67. AJ. 92:1364. doi:10.1086/114269.

Mathieu RD, Latham DW, Griffin RF. 1990. Orbits of 22 spectroscopic binaries in the open cluster M67. AJ. 100:1859. doi:10.1086/115643.

Mathieu RD, Latham DW, Griffin RF, Gunn JE. 1986. Precise radial velocities of late-type stars in the open clusters M11 and M67. AJ. 92:1100. doi:10.1086/114240.

Milone AAE. 1992. The Blue Stragglers of M67 and Other Open Clusters. PASP. 104:1268. doi:10.1086/133120.

Milone AAE, Latham DW. 1994. Radial velocities of blue stragglers. 1: a catalog of candidates in six open clusters. AJ. 108:1828. doi:10.1086/117195.

Monteiro H, Dias WS, Moitinho A, Cantat-Gaudin T, Lépine JRD, Carraro G, Paunzen E. 2020. Fundamental parameters for 45 open clusters with Gaia DR2, an improved extinction correction and a metallicity gradient prior. MNRAS. 499:1874M. doi:10.1093/mnras/staa2983.

Montgomery KA, Marschall LA, Janes KA. 1993. CCD photometry of the old open cluster M67. AJ. 106:181. doi:10.1086/116628.

Nardiello D, Libralato M, Bedin LR, Piotto G, Ochner P, Cunial A, Borsato L, Granata V. 2016. Variable stars in one open cluster within the Kepler/K2-Campaign-5 field: m 67 (NGC 2682). MNRAS. 455:2337. doi:10.1093/mnras/stv2439.

O'Donnell JE. 1994. R[SUB]nu[/SUB]-dependent optical and near-ultraviolet extinction. ApJ. 422:158. doi:10.1086/173713.

Pasquini L, Brucalassi, A, Ruiz, MT, Bonifacio, P, Lovis, C, Saglia, R, Melo, C, Biazzo, K, Randich, S, Bedin, LR, 2012. A&A. 545:A139. https://doi.org/10.1051/0004-6361/201219169

Pasquini L, Melo C, Chavero C, Dravins, D, Ludwig, HG, Bonifacio, P, De La Reza, R, 2011. A&A, 526. Preventing Chronic Disease. 8:A127.

Pearson AV, and Hartley HO. 1972. Biometrica Tables for Statisticians. Vol. 2, no. 4, 291. Cambridge (England): Cambridge University Press.

Percival SM, Salaris M, 2003, MNRAS, 343 539

Pribulla T, Rucinski S, Matthews JM, Kallinger T, Kuschnig R, Rowe JF, Guenther DB, Moffat AFJ, Sasselov D, Walker GAH, et al. 2008. MOST satellite photometry of stars in the M67 field: eclipsing binaries, blue stragglers and δ Scuti variables ★. MNRAS. 391:343. doi:10.1111/j.1365-2966.2008.13889.x.

Sanders WL. 1977. A&AS. Astron. Astrophys. Suppl. Ser. 27:89.

Sandquist EL, Shetrone MD. 2003a. Time series photometry of M67: w Ursae majoris systems, blue stragglers, and related systems. AJ. 125:2173. doi:10.1086/368139.

Sandquist EL, Shetrone MD. 2003b. S986 in M67: a totally eclipsing binary at the cluster turnoff. AJ. 126:2954. doi:10.1086/379175.

Spina L, Ting Y–S, De Silva GM, Frankel N, Sharma S, Cantat-Gaudin T, Joyce M, Stello D, Karakas AI, Asplund MB, et al. 2021. The GALAH survey: tracing the Galactic disc with open clusters. MNRAS. 503:3279. doi:10.1093/mnras/stab471.

Stassun KG, van den Berg M, Mathieu RD, and Verbunt F. February 2002. A&A. 382(3):899–909. https://doi.org/10.1051/0004-6361:20011737

Stello D, Arentoft T, Bedding TR, Bouzid MY, Bruntt H, Csubry Z, Dall TH, Dind ZE, Frandsen S, Gilliland RL, et al. 2006. Multisite campaign on the open cluster M67 – i. Observations and photometric reductions. MNRAS. 373:1141. doi:10.1111/j.1365-2966.2006.11060.x.

Stello D, Bruntt H, Kjeldsen H, Bedding TR, Arentoft T, Gilliland RL, Nuspl J, Kim S-L, Kang YB, Koo J-R, et al. 2007. Multisite campaign on the open cluster M67 - II. Evidence for solar-like oscillations in red giant stars. MNRAS. 377:584. doi:10.1111/j.1365-2966.2007.11585.x.

Stetson PB. 1987. DAOPHOT - A computer program for crowded-field stellar photometry. PASP. 99:191. doi:10.1086/131977.

Stetson PB. 1992. ASPC 25, Astronomical Data Analysis Software and Systems. Warrall DM, Biemesderfer C, and Barnes JI, ed. p. 297. Astronomical Society of Pacific.

Taylor BJ. 2007. The benchmark cluster reddening project. ii. A reddening value for m67. Astron. J. 133:370. doi:10.1086/509781.

van den Berg M, Stassun KG, Verbunt F, and Mathieu RD. 2002. A&A. 382:888–898.

Yadav RKS, Bedin LR, Piotto G, Anderson, J, Cassisi, S, Villanova, S, Platais, I, Pasquini, L, Momany, Y, Sagar, R, June 2008. A&A. 484(2):609.

Yakut K, Zima, W, Kalomeni, B, Van Winckel, H, Waelkens, C, De Cat, P, Bauwens, E, Vučković, M, Saesen, S, Le Guillou, L, et al. 2009. A&A. 503:165.

Zhao JL, Tian KP, Pan RS, He YP, and Shi HM. 1993. Astron. Astrophys. Suppl. Ser. 100:243–261.